# Supplementary Material for

# Exploring the direction-dependent of conductive filaments formation and oxygen vacancy migration behaviors in $HfO_2$-based RRAM

Donglan Zhang,[a] Jiong Wang,*[a] Qing Wu,[b] Yong Du[a]

[a]Powder Metallurgy Research Institute, Central South University, Changsha, Hunan, 410083, China

[b]Information and Network Center, Central South University, Changsha, Hunan, 410083, China

*E-mail address: wangjionga@csu.edu.cn

## Supplementary Note: Oxygen vacancy configurations for simulated conductive filaments formation

As observed experimentally[1, 2], the formation of oxygen vacancy conductive filaments (CFs) can be briefly described as follows: In the initial device, intrinsic vacancy defects in the materials are generated randomly, but can promote the formation of CFs. During the Forming process, more oxygen vacancies are gradually generated, which tend to form clusters and gradually accumulate from the cathode to the anode, eventually forming a CF that connects the two electrodes. The CFs are essentially a container for oxygen vacancies[3], which are distributed in a relatively orderly manner to form a CF connecting the top and bottom electrodes during the resistive switching process.

In other words, although the intrinsic oxygen vacancies are generated randomly in the initial device, during the Forming process, more oxygen vacancies will be generated around the intrinsic oxygen vacancies, which tend to accumulate in clusters and grow gradually from the cathode to the anode, eventually forming a CF connecting the top and bottom electrodes. In this work we focus on exploring the direction dependence in the formation of oxygen vacancy CFs. Considering that both relatively ordered and relatively disordered states of oxygen vacancy distribution are possible states in real devices, 13 configurations of ordered and disordered distribution of oxygen vacancies along different directions were established to simulate the formation of CFs, as shown

in Fig. 3 and Fig. S1. We have considered both the continuous and discontinuous distribution of oxygen vacancies along specific directions ([010] and [001]), as well as distribution of oxygen vacancies not along the [001] and [010] directions, but between 3-fold oxygen vacancy ($V_{O3}$) and 4-fold oxygen vacancy ($V_{O4}$) in *m*-$HfO_2$ system, to more reasonably simulate the possible states of the oxygen vacancy CFs formation during the resistive switching process. Regarding the oxygen vacancy configurations between $V_{O3}$ and $V_{O4}$, we have only considered the results of the partial charge density to reflect more visually the possible formation states of the CFs, as shown in Fig. S1.

Table S1 Wyckoff position of *m*-$HfO_2$

| Atom | Wyckoff positions |
|---|---|
| Hf | 4*e* (0.276, 0.041, 0.208) |
| O | 4*e* (0.073, 0.346, 0.332) |
| O | 4*e* (0.446, 0.748, 0.488) |

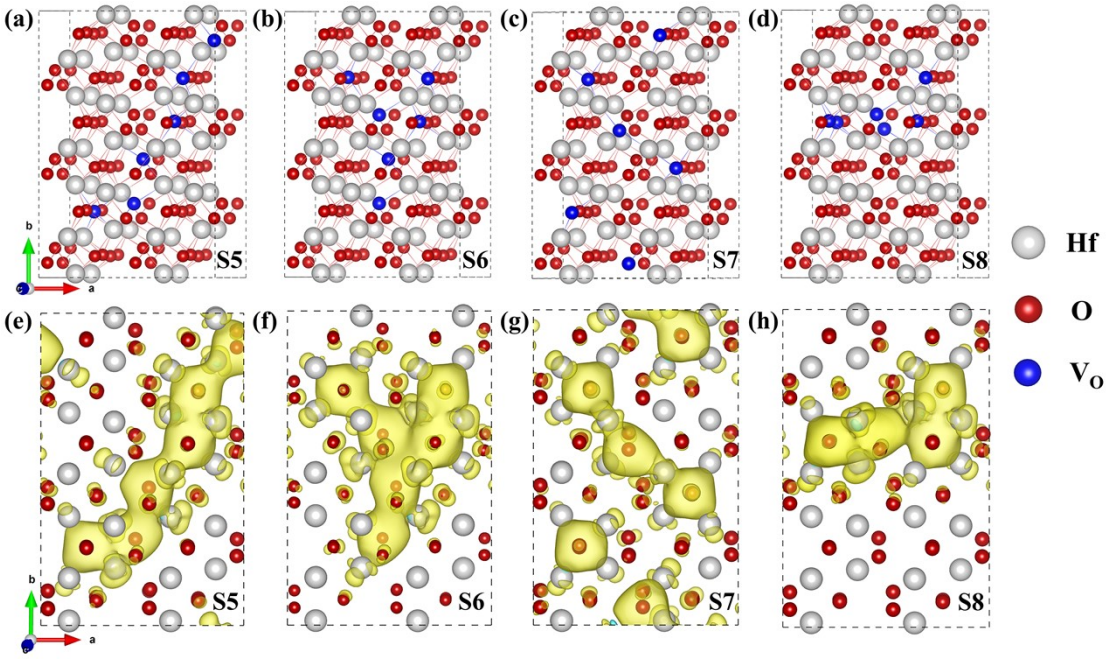


Fig. S1 The configurations of continuous and discontinuous distribution of 3-fold oxygen vacancy ($V_{O3}$) and 4-fold oxygen vacancy ($V_{O4}$) in the 2×3×2 *m*-$HfO_2$ supercell, corresponding to (a) S5. (b) S6. (c) S7 and (d) S8, respectively. The partial charge density Fig. (e)-(h) corresponding to configurations S5, S6, S7 and S8,

respectively.

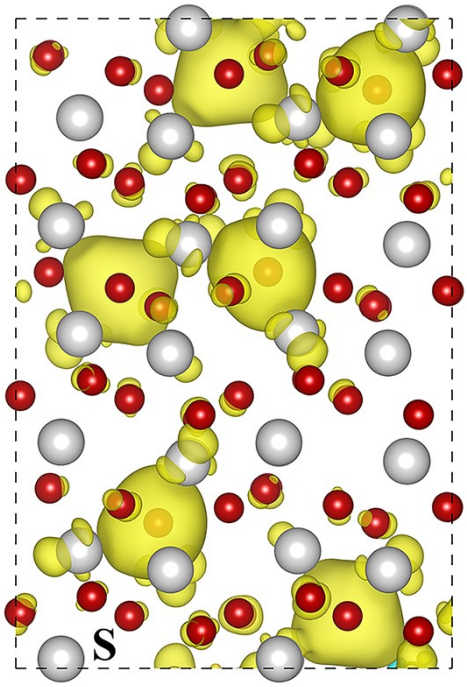


Fig. S2 The partial charge density of S ($V_{O3}$ and $V_{O4}$ discontinuous distribution at the (100) crystal plane in the *m*-$HfO_2$ supercell).

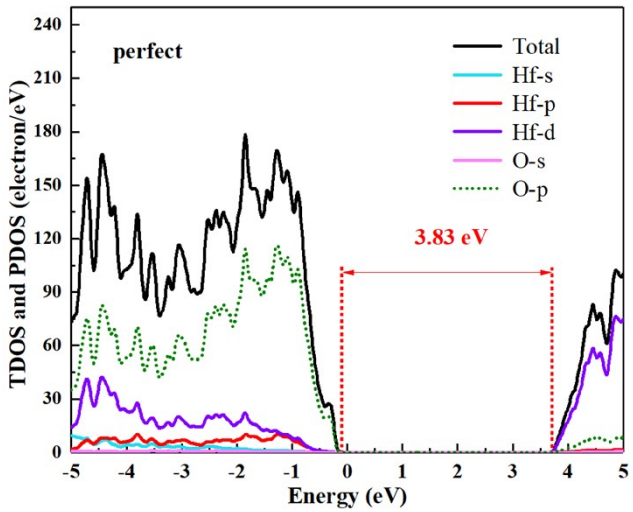


Fig. S3 The total density of states (TDOS) and partial density of states (PDOS) of perfect *m*-$HfO_2$ supercell without $V_O$.

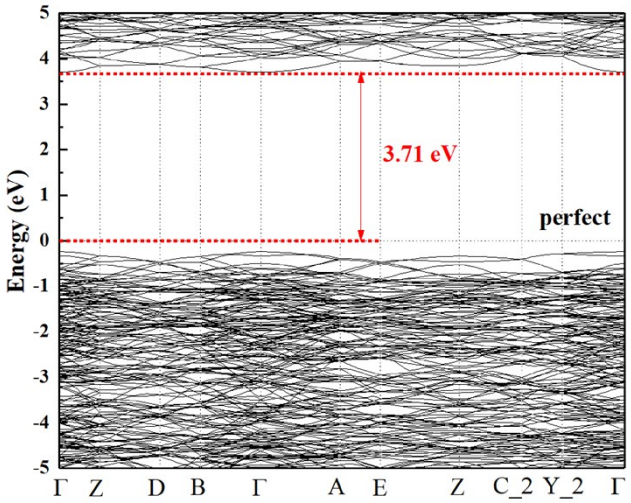


Fig. S4 The band structures of perfect *m*-$HfO_2$ supercell without $V_O$.

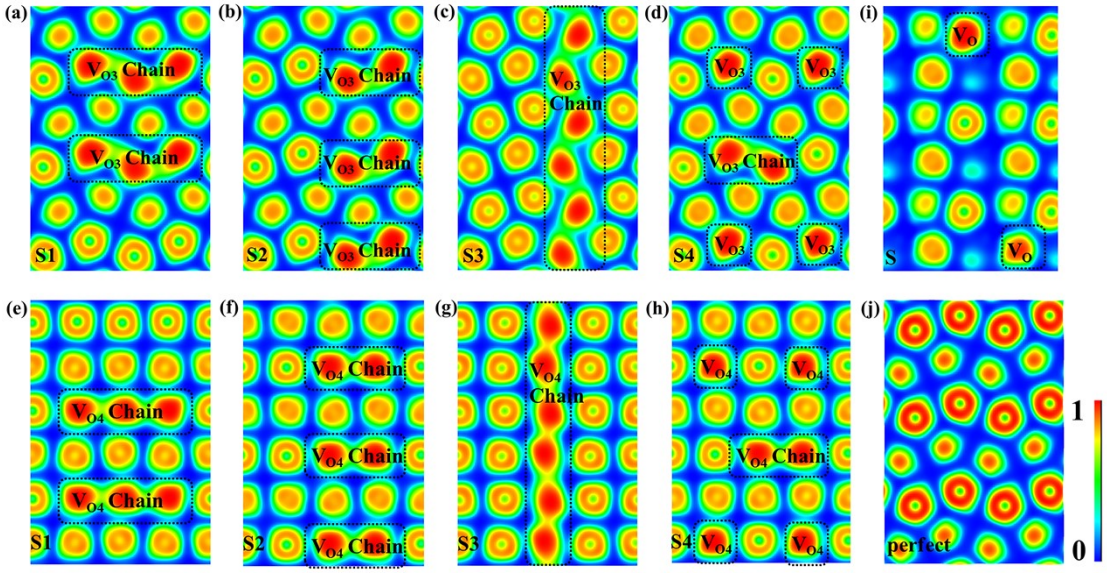


Fig. S5 The electron localization function (ELF) of continuous and discontinuous distribution of $V_{O3}$ and $V_{O4}$ at the (100) crystal plane in the 2×3×2 *m*-$HfO_2$ supercell. (a) S1-$V_{O3}$. (b) S2-$V_{O3}$. (c) S3-$V_{O3}$. (d) S4-$V_{O3}$. (e) S1-$V_{O4}$. (f) S2-$V_{O4}$. (g) S3-$V_{O4}$. (h) S4-$V_{O4}$. (i) S. (j) Perfect *m*-$HfO_2$ supercell without $V_O$.

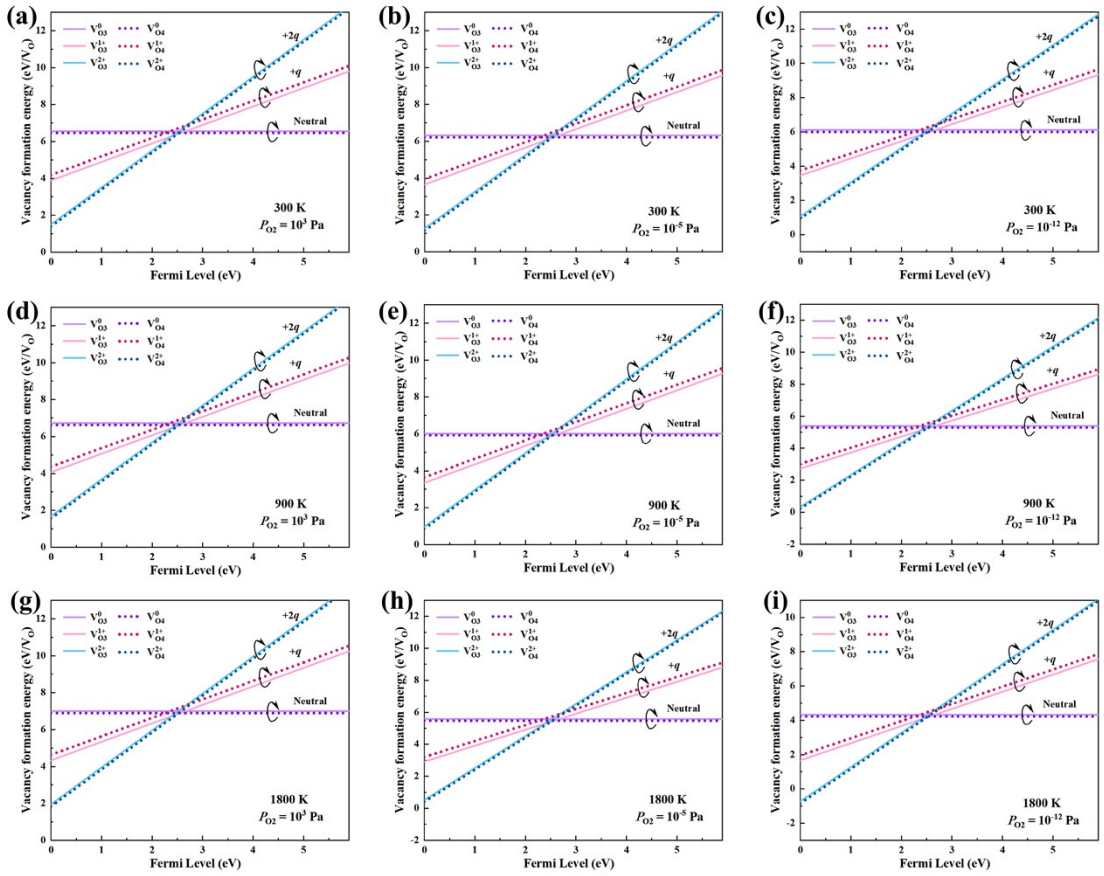


Fig. S6 The vacancy formation energy of S1-$V_{O3}$ and S3-$V_{O4}$ in the 2×3×2 *m*-$HfO_2$ supercell with charge states of 0, 1+ and 2+, respectively, as a function of Fermi level at different oxygen partial pressures and temperatures. Fig. (a)-(c), (d)-(f) and (g)-(i) shows vacancy formation energy in the same temperature (300, 900, and 1800 K) at different oxygen partial pressures, respectively.

## References


1 C. Li, B. Gao, Y. Yao, X. Guan, X. Shen, Y. Wang, P. Huang, L. Liu, X. Liu, J. Li, C. Gu, J. Kang and R. Yu, *Adv. Mater.*, 2017, **29**, 1602976.

2 Y. Zhang, G. Q. Mao, X. Zhao, Y. Li, M. Zhang, Z. Wu, W. Wu, H. Sun, Y. Guo, L. Wang, X. Zhang, Q. Liu, H. Lv, K. H. Xue, G. Xu, X. Miao, S. Long and M. Liu, *Nat. Commun.*, 2021, **12**, 7232.

3 U. Celano, L. Goux, R. Degraeve, A. Fantini, O. Richard, H. Bender, M. Jurczak and W. Vandervorst, *Nano Lett.*, 2015, **15**, 7970-7975.